Magnetotransport phenomena in $A(Mn_{3-x}Cu_x)Mn_4O_{12}$ (A=Ca, Tb, Tm) perovskites

I. O. Troyanchuk, L. S. Lobanovsky, and N. V. Kasper
Institute of Solid State and Semiconductor Physics, National Academy of Sciences of Belarus, P. Brovki Str. 17, 220072 Minsk, Belarus

M. Hervieu, A. Maignan, and C. Michel
Laboratoire CRISMAT, Bd du Maréchal Juin, 14050 Caen Cedex, France

H. Szymczak and A. Szewczyk
Institute of Physics, Polish Academy of Sciences, Al. Lotników 32/46, 02-668 Warsaw, Poland
(Received 17 June 1998)

The perovskites $Ca(Mn_{3-x}Cu_x)Mn_4O_{12}$ and $ACu_3Mn_4O_{12}$ (A=Tb, Tm) have been synthesized using different processes and their magnetic and transport properties investigated. $CaMn_3Mn_4O_{12}$ has been shown to be antiferromagnetic with T_N at approximately 85 K. This compound exhibits the resistivity drop more than one order of magnitude at 440 K due to the charge order-disorder transition. The substitution of manganese by copper leads to ferrimagnetic state developing through intermediate spin glass state. A clear increase of both T_C and magnetization value at low T is observed as the copper content increases up to $x=1.5$. For this particular $x=1.5$ composition, a metal-insulator transition is observed at 160 K, whereas for smaller Cu content a semiconducting behavior is exhibited. The Ca-free samples $TbCu_3Mn_4O_{12}$ and $TmCu_3Mn_4O_{12}$ are also ferrimagnets exhibiting a metal-like behavior below 360 K and a metal-insulator transition at 250 K for the former and the latter, respectively. But the most interesting result deals with the magnetoresistance (MR) of all the ferrimagnetic samples that can reach up to 20% in 1 T at 77 K. The appearance of this MR is closely related to the antiferromagnetic Cu-Mn interactions development and, in contrast to colossal MR perovskites, its value is no more maximum at T_C but it increases continuously as T decreases. [S0163-1829(98)00246-X]

I. INTRODUCTION

Recently a great deal of attention has been focused on the magnetoresistance MR of manganese perovskites with chemical formula $La_{1-x}A_xMnO_3$ where A=Ca, Ba, Sr due to their potential magnetoresistance properties.[1–6] Besides these compounds, there exists another class of perovskites with the general formula $AC_3B_4O_{12}$, firstly observed for $CaCu_3Ti_4O_{12}$,[7] characterized by an ordering of the interpolated cations due to the Jahn-Teller effect of copper. The manganites $AC_3Mn_4O_{12}$ (A=Ca, lanthanide ion; C=Mn, Cu) synthesized under high pressure[8,9] represent potential materials for the magnetoresistance effect, owing to the simultaneous presence of Mn^{3+} and Mn^{4+} species. $[AMn_3]Mn_4O_{12}$ is rhombohedral (space group $R\bar{3}$). The authors of the work[8] believe the ionic ordering of Mn^{3+} and Mn^{4+} to be the cause of the symmetry lowering. This compound at $T=440$ K undergoes first-order phase transition into cubic phase apparently due to charge ordering.[9] While substituting the Cu^{2+} by Mn^{3+} in the C sublattice, an equivalent quantity of the Mn^{4+} ions in the B sublattice passes over to Mn^{3+}. According to Ref. 10 $Ca(Mn_{0.66}Cu_{2.34})Mn_4O_{12}$ is a noncollinear ferrimagnet with $T_C=350$ K. For $ThCu_3(Mn_2^{3+}Mn_2^{4+})O_{12}$ compound the Curie temperature reaches 430 K.[10] Magnetic properties are governed by the strong antiferromagnetic superexchange between copper and manganese ions located in C and B sublattices, respectively.[11] In spite of interesting magnetic properties, there is no magnetotransport data in the literature. The present work aims at investigating the $A(Mn_{3-x}Cu_x)Mn_4O_{12}$ system. Two types of synthesis, under high pressure ($P=5$ GPa) as reported in the previous works,[9,10] or normal pressure, were used. The magnetic and magnetotransport properties were characterized, depending on the synthesis process and on the Mn^{3+}/Mn^{4+} ion ratio in the B sublattice.

II. EXPERIMENT

Three different kinds of procedures were used for the synthesis of materials:

(i) Starting from stoichiometric mixtures of $CaCO_3$, $Mn(OH)_3$, and $Cu(OH)_2$, the synthesis can be performed in air at 1070 K using conventional ceramic technology. By this method $Ca(Mn_{3-x}Cu_x)Mn_4O_{12}$ samples can be prepared up to $x=1.10$. (ii) Starting from stoichiometric mixtures of nominal composition ''1 CaO, x CuO, 5 MnO_2, $(1-x/2)$ Mn_2O_3,'' pressed in the form of bars, the synthesis is performed in evacuated silica tubes at 1370 K for 48 h. By this method, the limit composition $x=1.50$ can be reached. (iii) The samples with $x>1.1$ and $ACu_3Mn_4O_{12}$ (A=Gd,Tb,Tm) can also be obtained by a solid-state reaction under high pressure and temperature ($P=5$ GPa and $T=1570$ K).

We could not obtain a sample of $Ca(Mn_{0.8}Cu_{2.2})Mn_4O_{12}$ composition without cracks using this method. This sample was ground after synthesis and cold pressed at $P=5$ GPa in order to measure electrical conductivity.

Magnetotransport measurements have been carried out using a standard four-probe dc method. The magnetization and magnetic hysteresis loops have been measured using a Foner vibrating sample magnetometer.

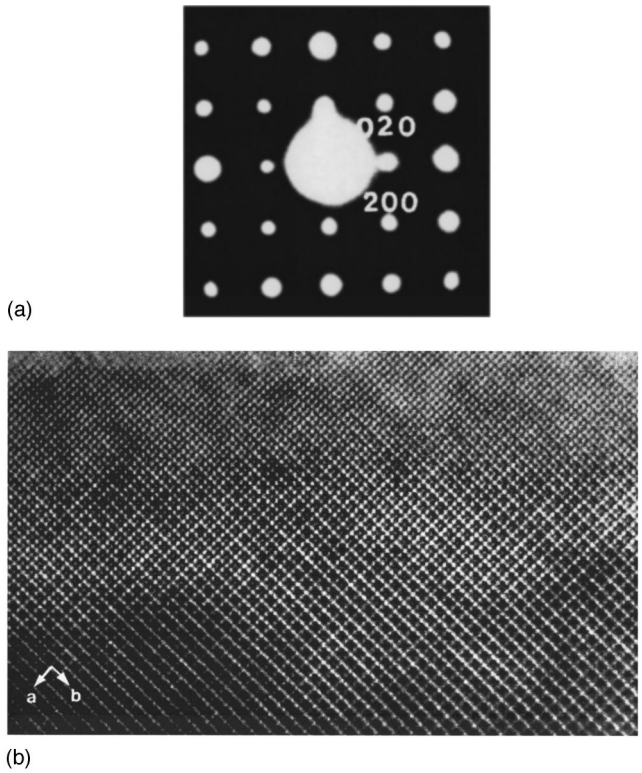

FIG. 1. (a) [100] ED pattern of the cubic $Ca(Mn_2Cu)Mn_4O_{12}$ phases; (b) [100] HREM: a very regular contrast is observed, which perfectly fits with the theoretical images. The theoretical image is calculated for a crystal thickness of 22 Å and a focus value of ~650 Å. No defect was detected.

The samples for electron microscopy were prepared by crushing the crystals in alcohol. The flakes were deposited on a holey carbon film supported by a nickel grid. The electron diffraction (ED) study was carried out using a JEOL 200 CX electron microscope fitted with a eucentric goniometer ($\pm 60°$). The high-resolution electron microscopy (HREM) was performed with a TOPCON 002B operating at 200 KV (spherical aberration constant Cs = 0.4 mm). HREM images calculations were carried out with the Mac-Tempas multislice program. The two microscopes are equipped with EDX analyzers.

The powder x-ray diffraction (XRD) data were collected with a Philips vertical diffractometer (Cu Kα radiation) in the range $10° < 2\Theta < 110°$ by increment of 0.02 (2Θ). Cell parameters and structure calculations were performed by profile analysis (program Fullprof version 3.2).[12]

III. RESULTS AND DISCUSSION

A. Structural characterization

Working under air at 1070 K, the existence range of the solid solution $Ca(Mn_{3-x}Cu_x)Mn_4O_{12}$ is $0 \leqslant x \leqslant 1.1$. According to the x-ray analysis some samples contain very small admixtures of unreacted oxides being less than 3%, however.

Working under oxygen pressure at 1370 K in sealed tubes, the existence range is $0 \leqslant x \leqslant 1.5$. The EDS analyses performed on numerous grains showed that the Ca/Cu/Mn ratio is highly constant and that the actual compositions are very close to the nominal ones.

TABLE I. $A(Mn_{3-x}Cu_x)Mn_4O_{12}$: cell parameters.

Composition	Lattice[a]	a (Å)	α (°)
	1070 K air		
$CaMn_3Mn_4O_{12}$	Rh	7.377(1)	90.39
$Ca(Mn_{1.9}Cu_{1.1})Mn_4O_{12}$	C	7.310(1)	
	1370 K oxygen		
$CaMn_3Mn_4O_{12}$	Rh	7.369(1)	90.36
$Ca(Mn_{2.5}Cu_{0.5})Mn_4O_{12}$	C	7.344(2)	
$Ca(Mn_2Cu_1)Mn_4O_{12}$	C	7.323(1)	
$Ca(Mn_{1.5}Cu_{1.5})Mn_4O_{12}$	C	7.309(1)	
	1570 K 5 GPa		
$Ca(Mn_{2.2}Cu_{0.8})Mn_4O_{12}$	C	7.254(1)	
$TbCu_3Mn_4O_{12}$	C	7.258(1)	
$TmCu_3Mn_4O_{12}$	C	7.247(1)	

[a]C, cubic, Rh, rhombohedral.

The reconstruction of the reciprocal space was carried out by tilting around the crystallographic axes of the perovskite subcell. The electron diffraction study confirms that the cell parameters are twice the a_p parameter of the ideal perovskite. The $Ca(Mn_{3-x}Cu_x)Mn_4O_{12}$ samples with $x \neq 0$ are cubic whereas the Cu-free sample, $CaMn_3Mn_4O_{12}$, exhibits a rhombohedral distortion. The conditions limiting the reflection are hkl: $h+k+l=2n$, leading to the space groups $I23$ or $Im3$ for the cubic phases and $R3$ or $R\bar{3}$ for the rhombohedral one, in agreement with Ref. 8. The [100] ED pattern of $CaMn_3Mn_4O_{12}$ is given in Fig. 1(a).

The unit-cell parameters of the different samples (Table I) were refined from powder x-ray diffraction patterns (Fig. 2). The structure of $Ca(Mn_2Cu)Mn_4O_{12}$ was refined in the space group $Im3$, starting from the results previously obtained for $CaCu_3Mn_4O_{12}$.[13] Copper was statistically distributed with a part of manganese over the 6b crystallographic sites. Positional parameters of oxygens and isotropic temperature factors for all atoms were successively refined. Convergence was obtained for the values listed in Table II, leading to a R_B factor of 7%.

The high-resolution electron microscopy was carried out on the $Ca(Mn_2Cu)Mn_4O_{12}$ sample. This study shows that all

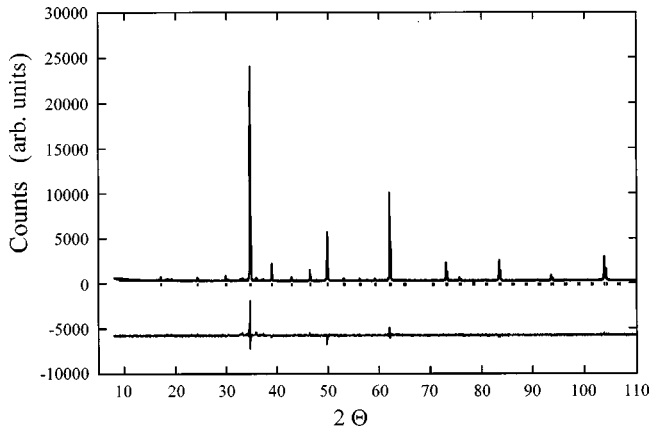

FIG. 2. Experimental and difference XRD patterns of $Ca(Mn_2Cu)Mn_4O_{12}$ (sticks represent the Bragg angle positions).

TABLE II. $Ca(Mn_2Cu)Mn_4O_{12}$, $a=7.3230(1)$ Å, space group $Im3$; $R_P=0.071$; $R_{WP}=0.094$; $R_B=0.072$.

Atom	Site	x	y	z	B (Å^2)
Ca	2a	0	0	0	1.5(4)
Cu/Mn	6b	0	1/2	1/2	0.5(1)
Mn	8c	1/4	1/4	1/4	0.1(1)
O	24g	0	0.178(1)	0.310(1)	1.3(2)

the crystallites exhibit a very regular contrast. One example of [100] HREM image is given in Fig. 2(b). The theoretical images calculated from the refined positional parameters (Table II) fit with the experimental one. No pointlike nor extended defect have been detected.

Thus, the structure of $Ca(Mn_2Cu)Mn_4O_{12}$ is like that of $CaCu_3Mn_4O_{12}$ characterized by diamond shaped tunnels (Fig. 3), in which the Ca^{2+} cations, Cu^{2+} and Mn^{3+} cations exhibit a particular coordination.

The Ca^{2+} are surrounded by twelve equidistant oxygens (2.62 Å), whereas Cu^{2+} and Mn^{3+} cations, thanks to the Jahn-Teller effect exhibit a 4 + 4 + 4 coordination: four oxygen at short distances (1.91 Å) form a square, the second neighbors form a rectangle (2.74 Å), and, lastly, the four farthest oxygens are at 3.27 Å. In the $Im3$ space group, only one site is available for the Mn located in the octahedral sites (B sites of the perovskite), so that no order phenomenon is considered between Mn^{3+} and Mn^{4+}. The six Mn-O distances are at 1.95 Å.

B. Magnetotransport properties

The undoped sample $CaMn_3Mn_4O_{12}$, which is rhombohedral, does not show any spontaneous magnetization in the whole (293–4.2 K) temperature range (Fig. 4). This sample shows anomalous magnetization behavior at approximately

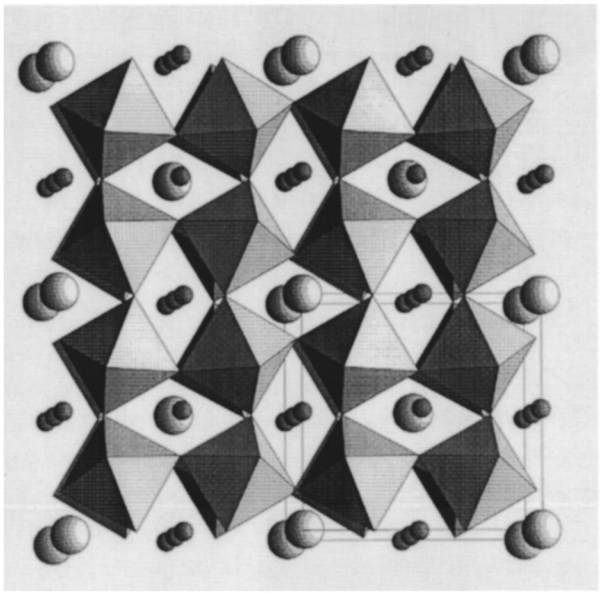

FIG. 3. Schematic drawing of the structure of $Ca(Mn_2Cu)Mn_4O_{12}$ showing the diamond-shaped tunnels where are located calcium (large spheres), Cu^{2+}, and Mn^{3+} (small spheres).

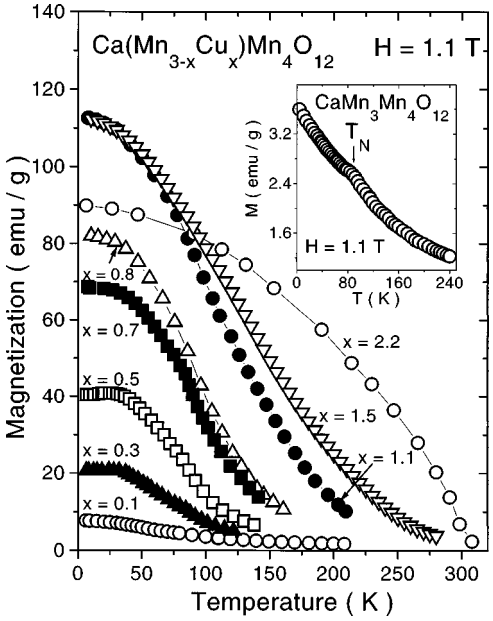

FIG. 4. Magnetization vs temperature for $Ca(Mn_{3-x}Cu_x)Mn_4O_{12}$ compounds.

85 K. This anomaly could be associated with Néel temperature. Spontaneous magnetization develops in copper substituted samples (Fig. 4). The sample $x=0.5$ shows a peak of field cooled magnetization at approximately 35 K. The field of 11 kOe is not enough to suppress this phenomenon. Below 35 K the magnetization depends strongly on the magnetic prehistory. The magnetic properties indicate cluster spin-glass state. The spontaneous magnetization of $Ca(Mn_{3-x}Cu_x)Mn_4O_{12}$ increases as x increases, reaching 110 emu/g or 13 μ_B per formula unit for $x=1.5$. This value corresponds to antiferromagnetic ordering of manganese in the B sublattice and copper magnetic moments taking into account possible noncollinear magnetic structure as it was observed earlier for a $x=2.34$ sample by the neutron diffraction method.[10] Further Cu-content increase leads to decreasing spontaneous magnetization whereas the Curie point increases up to 360 K for $Ca(Mn_{0.5}Cu_{2.5})Mn_4O_{12}$ or 380 K for the $TbCu_3Mn_4O_{12}$ compound. Spontaneous magnetization corresponds to opposite alignment of magnetic moments of copper and manganese ions. Such a behavior could be attributed to strong negative exchange interactions between Cu and Mn ions. The magnetic properties of $ACu_3Mn_4O_{12}$ (A = Tb,Gd,Tm) are similar. All these compounds are ferrimagnets with T_C close to 380 K.

The electrical resistivity behavior is displayed in Fig. 5. $CaMn_3(Mn_3^{3+}Mn^{4+})O_{12}$ exhibits a drop of resistivity more than one order of magnitude at around 440 K (see inset to Fig. 5). This anomaly is likely associated with the charge ordering phenomenon. At 440 K the symmetry of the lattice changes from rhombohedral to cubic, as it was found in Ref. 9. The high-temperature phase is nonmetallic with activation energy of charge carriers close to 0.08 eV. The substitution of manganese by copper leads to a strong decrease of resistivity, so that a metal-insulator transition is finally observed for $Ca(Mn_{1.5}Cu_{1.5})Mn_4O_{12}$ ($x=1.5$) [see also Fig. 6(a)]. The appearance of such a transition is in perfect agreement with the facts that the magnetization is the highest for this com-

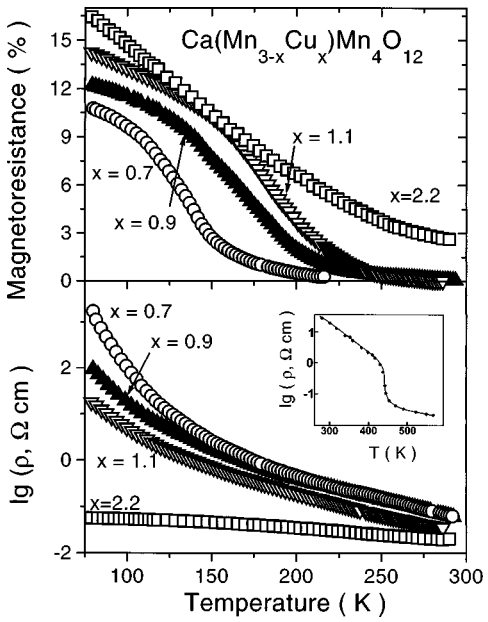

FIG. 5. Magnetoresistance and resistivity vs temperature behavior for $Ca(Mn_{3-x}Cu_x)Mn_4O_{12}$ samples. The inset shows the drop of resistivity in $CaMn_3(Mn_3^{3+}Mn^{4+})O_{12}$ around the charge ordering transition.

position and that crystal structure distortions are completely removed owing to change ordering. The $Ca(Mn_{0.8}Cu_{2.2})Mn_4O_{12}$ sample does not exhibit metallic behavior (Fig. 5). The resistivity is slightly dependent on the temperature. Such a behavior could be attributed to the method of preparation of this sample because NMR data indicate similar signals from manganese ions in the whole $1.1 < x < 2.5$ composition range.[14] $TbCu_3Mn_4O_{12}$ shows a metallic behavior in the whole investigated range of temperature ($10 < T < 380$ K) [Fig. 6(b)]. This compound contains approximately 25% of trivalent manganese ions in the manganese sublattice. It is worth to be noted that manganites with chemical formula $La^{3+}_{1-x}A^{2+}_xMnO_3$ (where A = Ca,Ba,Sr) show a strongly insulating behavior in this range of three-valent manganese concentrations.[15,16]

The $\rho(T)$ curves registered under 0 and 1 T show that the all Cu-containing manganites $Ca(Mn_{3-x}Cu_x)Mn_4O_{12}$ [Figs. 5,6(a)], $TbCu_3Mn_4O_{12}$ [Fig. 6(b)] and $TmCu_3Mn_4O_{12}$ [Fig. 6(c)] exhibit MR. For the lowest temperature, the value of the latter defined as

$$MR = [\rho(H=0) - \rho(H=1T)]*100\%/\rho(H=0)$$

is rather small, i.e. smaller than 15% and rather comparable with that observed for the perovskite $La_{0.6}Pb_{0.4}MnO_3$ [Fig. 6(d)]. In all the $A(Mn_{3-x}Cu_x)Mn_4O_{12}$ phases the MR starts to increase at around Curie temperature and increases gradually with decreasing temperature. The increase of MR with the increasing of Cu content (Fig. 5) is in good agreement with enhancement of magnetization due to concentrational antiferromagnet-ferromagnet transition. In contrast to well-known manganites $La_{1-x}A_xMnO_3$ we have not observed any peak of MR at around T_C as shown for bulk polycrystalline samples of $La_{0.6}Pb_{0.4}MnO_3$ in a field of 1 T [Fig. 6(d)]. It is clearly seen that the behavior of $TbCu_3Mn_4O_{12}$ [Fig. 6(b)] is similar to $La_{0.6}Pb_{0.4}MnO_3$ at low temperature, near 77 K, whereas the data differ markedly near T_C. However, the magnetic structure of both compounds is different: $TbCu_3Mn_4O_{12}$ is ferrimagnet with antialigned copper and manganese magnetic moments whereas $La_{0.6}Pb_{0.4}MnO_3$ is ferromagnet; furthermore the concentration of Mn^{4+} ions in Tb-based compound is 75%, whereas in La-based one it is only 40%.

The transport behavior of $TmCu_3Mn_4O_{12}$ [Fig. 6(c)] and of $Ca(Mn_{1.5}Cu_{1.5})Mn_4O_{12}$ [Fig. 6(a)] is characterized by a metal-insulator transition at 260 and 160 K, respectively. In

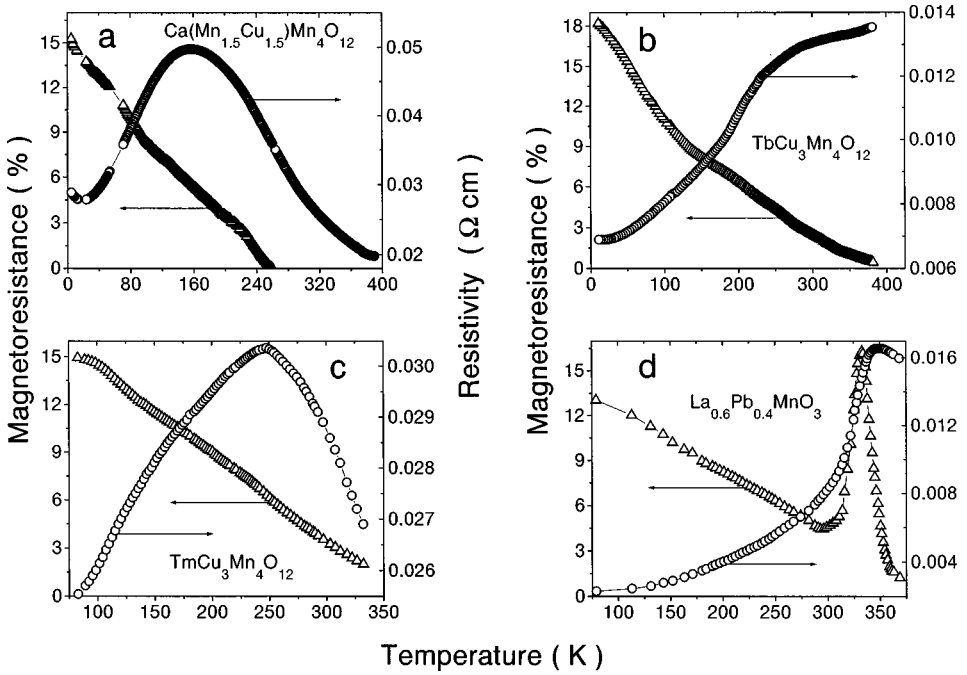

FIG. 6. Resistivity and magnetoresistance vs temperature for $Ca(Mn_{1.5}Cu_{1.5})Mn_4O_{12}$ (a), $TbCu_3Mn_4O_{12}$ (b), $TmCu_3Mn_4O_{12}$ (c), and $La_{0.6}Pb_{0.4}MnO_3$ (d).

both oxides no peak of MR is observed. The MR increases gradually with decreasing temperature, starting from Curie point and reaches 15% and 12%, respectively, in a field of 1 T at 77 K.

In contrast to the well-known $(La,Ca)MnO_3$ manganites the Mn-O-Mn angle in the $AC_3B_4O_{12}$ series is slightly dependent on size of *A*, *C*, and *B* ions and remains close to 140^0 not depending on composition.[10,17] In this case, an appreciable narrowing of the conduction band due to decreasing of the lanthanide size is not expected. It is well known that metallic $(La,Ca)MnO_3$ exhibit intermediate manganese valence whereas NMR study of $Ca(Mn_{3-x}Cu_x)MnO_{12}$ has not revealed this phenomenon.[14] Hence, further investigation is needed to understand the nature of metal-insulator transition in $AC_3Mn_4O_{12}$ compounds.

The MR data received here on $AC_3Mn_4O_{12}$ compounds resembles those for polycrystalline samples of Fe_3O_4 spinel[18] and CrO_2 rutile.[19] In Fe_3O_4 and CrO_2 the magnetoresistance arises from misaligned magnetization in adjacent ferromagnetic grains that are exchange decoupled. In order to explain the temperature dependence of the magnetoresistance the authors of work[18] suggest a simple model in which two types of charge carriers traverse a grain boundary: those that hop in a number of steps and a smaller part that tunnels across in one step between the conduction bands of the two grains. The latter are main charge carriers at low temperatures and would conserve their spin in a single jump. The charge carriers traversing a grain boundary in many steps have time to relax their spin reorientation between jumps and cannot contribute to giant magnetoresistance effect.

It is necessary to note that intergranular magnetoresistive effect in $ACu_3Mn_4O_{12}$ ferrimagnets is much larger than that in Fe_3O_4 ferrimagnet. The magnitude of the intergranular magnetoresistance in $ACu_3Mn_4O_{12}$ compounds is comparable to that for $La_{1-x}A_xMnO_3$ manganites[20] in spite of different magnetic structures and mechanisms of exchange interactions.

ACKNOWLEDGMENTS

This work was supported partly by the Belarus Fund for Fundamental Researches (Grant No. F96-135) and Polish State Committee for Scientific Researches (Grant No. 2 PO3 B 095 12).

[1] R. von Helmot, J. Wecker, B. Holzapfel, L. Schultz, and K. Samwer, Phys. Rev. Lett. **71**, 2331 (1993).
[2] K. Chahara, T. Ohno, M. Kasai, and Y. Kozono, Appl. Phys. Lett. **63**, 1990 (1993).
[3] S. Jin, H. M. O'Bryan, T. H. Tiefel, M. Mc Cormack, and W. W. Rodes, Appl. Phys. Lett. **66**, 382 (1994).
[4] Y. Tomioka, A. Asamitsu, Y. Moritomo, H. Kuwahara, and Y. Tokura, Phys. Rev. Lett. **74**, 5108 (1995).
[5] H. L. Ju, C. Kwon, R. L. Greene, and T. Venkatesan, Appl. Phys. Lett. **65**, 2108 (1994).
[6] B. Raveau, A. Maignan, and Ch. Simon, J. Solid State Chem. **117**, 424 (1995).
[7] A. Deschanvres, B. Raveau, and F. Tollemer, Bull. Chem. Soc. Jpn. **11**, 4071 (1967).
[8] B. Bochu, J. L. Buevoz, J. Chenavas, A. Collomb, J. C. Joubert, and M. Marezio, Solid State Commun. **36**, 133 (1980).
[9] I. O. Troyanchuk, L. V. Balyko, and L. A. Bashkirov, Cryst. Res. Technol. **21**, 705 (1986).
[10] A. Collomb, D. Samaras, J. Chenavas, M. Marezio, J. C. Joubert, B. Bochu, and M. N. Deschizeaux, J. Magn. Magn. Mater. **7**, 1 (1978).
[11] I. O. Troyanchuk, A. S. Chernyi, and E. F. Shapovalova, Phys. Status Solidi A **112**, 155 (1989).
[12] J. Rodriguez-Carvajal (unpublished).
[13] B. Bochu, J. Chenavas, J. C. Joubert, and M. Marezio, J. Solid State Chem. **11**, 88 (1974).
[14] I. O. Troyanchuk, L. A. Bashkirov, A. A. Shemyakov, and V. K. Prokopenko, Phys. Status Solidi A **109**, 59 (1988).
[15] A. Barnabe, A. Maignan, M. Hervieu, and B. Raveau, Eur. Phys. J. B **1**, 145 (1998).
[16] I. O. Troyanchuk, N. V. Kasper, N. V. Samsonenko, H. Szymczak, and A. Nabialek, J. Phys.: Condens. Matter **8**, 10 627 (1996).
[17] M. N. Deschizeaux and J. C. Joubert, J. Solid State Chem. **19**, 45 (1976).
[18] J. M. D. Coey, A. E. Barkowitz, L. Balsells, F. F. Patris, and F. T. Parker, Appl. Phys. Lett. **72**, 734 (1998).
[19] S. Manoharam, D. Elefant, G. Reiss, and J. B. Goodenough, Appl. Phys. Lett. **72**, 984 (1998).
[20] X. W. Li, A. Gupta, G. Xiao, and G. Q. Gong, Appl. Phys. Lett. **71**, 1124 (1997).